Wall Thickness Loss Estimation Based on Acoustic Emission in Steel Structures

ROMAIN HABIYAREMYE, ARJAN MOL,
HARLEIGH SEYFFERT and LOTFOLLAH PAHLAVAN

ABSTRACT

Corrosion is a leading damage mechanisms in the degradation of marine assets. Acoustic emission (AE) monitoring has gained increasing interest as a technique for continuous monitoring of corrosion damage. This study numerically and experimentally investigates the feasibility of wall thickness loss estimation from the AE signals due to localized corrosion. The interaction of the elastic waves emitted due to the evolution of corrosion damage are influenced by the local thickness and material properties of the structure. A steel plate of (500 mm x 500 mm x 10 mm) with a localized wall thickness loss between 0 and 80% in the center of the plate was considered. The numerical investigation was conducted using a higher-order finite element model. Laboratory experiments were performed on a carbon steel specimen instrumented with 7 AE transducers (40 - 250 kHz). Corrosion damage was artificially introduced in the steel plate by progressively milling a pit in the center. At different stages of wall thickness loss, simulated AE sources were generated. The response of the structure was evaluated based on signal characteristics such as amplitude, rise-time, frequency content, and waveform. A correlation between the signal amplitudes and the wall thickness loss was observed in both experimental and numerical results. This perspective is promising for the feasibility of corrosion-induced wall thickness loss estimation based on AE measurements.

INTRODUCTION

Corrosion is one of the main driving mechanisms that lead to failure in marine and offshore assets [1–3]. Traditional non-destructive testing methods used for inspections are very localized and therefore, labor-intensive at the scale of full-sized structures such as ship hulls. Lengthy inspection campaigns are, in addition to being inherently expensive, keeping assets out of service for extended periods of time. The maritime industry has, for these reasons, a growing interest in structural health monitoring and predictive maintenance. In light of these developments, classification societies have started to incorporate hull monitoring systems in their guidelines [4–6].

Romain Habiyaremye, PhD Candidate, Email: R.Habiyaremye@tudelft.nl. Ship and Offshore Structures section, Department of Maritime and Transport Technology, Delft University of Technology, Delft, The Netherlands

Acoustic emission (AE) monitoring is a structural health monitoring technique that offers the possibility of detecting a multitude of different damage mechanisms such as fatigue, creep, and corrosion [7–11]. AE monitoring consists in measuring elastic stress waves caused by a rapid release of energy when irreversible changes occur in a material [12]. In thin-walled structures, these stress waves propagate as guided waves and can be detected and measured by a distributed network of piezoelectric sensors. AE signals can originate from corrosion-related effects such as hydrogen bubble activity, passive film rupture, and pit growth [9, 13–15]. Acoustic emission techniques allow for the detection and localization of the onset and progression of damage in many types of marine and offshore structures such as ship hulls, mooring chains, and offshore jackets [16–19]. The estimation of the remaining wall thickness is a critical step in the context of predictive maintenance. Active methods for wall thickness measurements techniques are well established [20–24]. More recent research by Reed and Corconan [25] investigates passive wall thickness monitoring through resonant ultrasound spectroscopy and time of flight measurements. These methods, however, only allow for localized measurement at the location of the ultrasonic transducer. The utilization of inverse FEM has been studied by Silionis and Anyfantis [26] based on local strain measurements. The strain measurements could be used to reconstruct the entire stress field and infer a generalized wall thickness loss in plates of a ship hull due to uniform corrosion. There is a need for further development of techniques that allow for passive corrosion-induced thickness loss estimation beyond the location of SHM sensors.

This paper investigates the feasibility of the estimation of local wall thickness loss in steel plates based on acoustic emission signal characteristics. Numerical modeling of elastic wave propagation has been used to simulate and study the response to high frequency AE in a steel plate under different stages of progressing corrosion damage. Experiments have also been executed by subjecting a carbon steel plate to simulated AE excitation by means of a Hsu-Nielsen source. Controlled wall thickness loss has been introduced by milling a hole in the center of the steel sample. AE excitations have been applied at each stage of increased damage. The results from both the experimental results and the numerical model indicate a correlation between the depth of the damage and the amplitude of the signals. This is promising for the estimation of corrosion-induced wall thickness loss based on AE monitoring.

METHODOLOGY

The energy liberated by the development of a given damage mechanism will be, in part, converted in elastic waves that can propagate through the material of the structure. This propagation can be either in the form of bulk waves, surface waves, or guided waves, depending on the geometry of the medium and the frequency of the waves [27]. Damage-induced AE signals propagate as guided waves in thin-walled structures such as ship hulls. A given measured signal P can be modeled as the result of the convolution of the source signal S with the transfer function of the wave propagation through the structure W and the transfer function of the measurement system (i.e. sensor, preamplifier, and data acquisition system), denoted D. This convolution is summed over all wave modes i. A certain amount of noise N is expected from external sources as shown in equation 1.

thickness	length,width	density	elastic modulus	Poisson's ratio
10 mm	500 mm	7800 kg/m^3	207 GPa	0.33

TABLE I. material properties applied in the finite element model

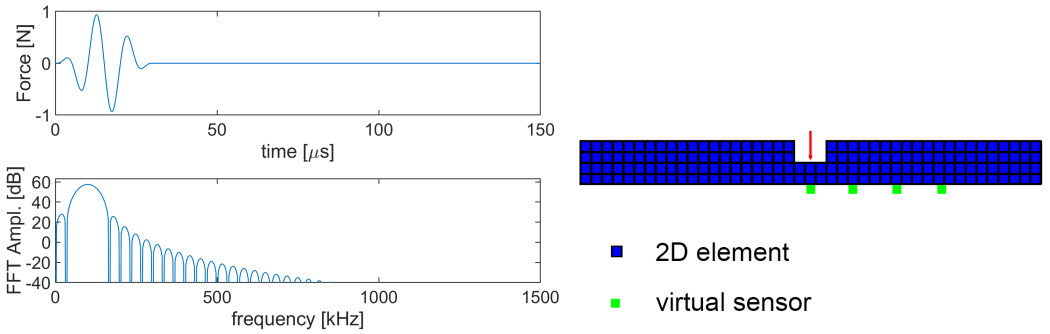

(a) Input force signal

(b) Schematic cross section view of the numerical model

Figure 1. Finite element analysis mode

$$P = \sum_{i=1}^{n} D_i W_i S_i + N \tag{1}$$

As damage develops in the structure, it can be expected that the local source-related term S may change. Assuming that the other terms in the equation remain constant, this study investigates how the remaining wall thickness of a localized corrosion site might affect the measured signals P.

Numerical model

The second-order spectral element method (SEM) has been used to study the behavior of AE signals under varying damage conditions [28–32]. The model uses second-order 2D elements for improved accuracy in high-frequency stress wave modeling. A 150 kHz force excitation was applied to the center of the plate as shown in figure 1. A steel plate with dimensions of 500 mm x 500 mm x 10 mm was chosen based on preliminary calculations, primarily to leave space between input signals and boundary reflections. An element size of 1 mm was chosen to model the plate, resulting in 5000 solid elements. The material properties applied to the model are listed in table I. A time step of 0.1 µs has been selected to take the high-frequency displacements into account. The transient response was obtained using an explicit Newmark integration method. Corrosion damage was simulated by introducing a cavity in the surface of the plate with a diameter of 15 mm. The AE behavior was simulated for an intact plate and increased depths of local damage of 2, 4 mm up to 6 mm. An excitation is applied to the structure in the form of a 150 kHz force pulse signal (3-cycle Hanning-windowed sinusoidal signal) with an amplitude of 1 N in the center (see figure 1). The surface elevation was evaluated at different locations along the opposite side of the excitation force.

Experiments

model	Sensor type	Operating range	f_{peak}	Pass-band
R6α	Narrow band	35-100 kHz	55 kHz	40-100 kHz
R15α	Narrow band	50-400 kHz	75 kHz	95-180 kHz

TABLE II. Sensor specifications and band-pass filter pass-band frequencies

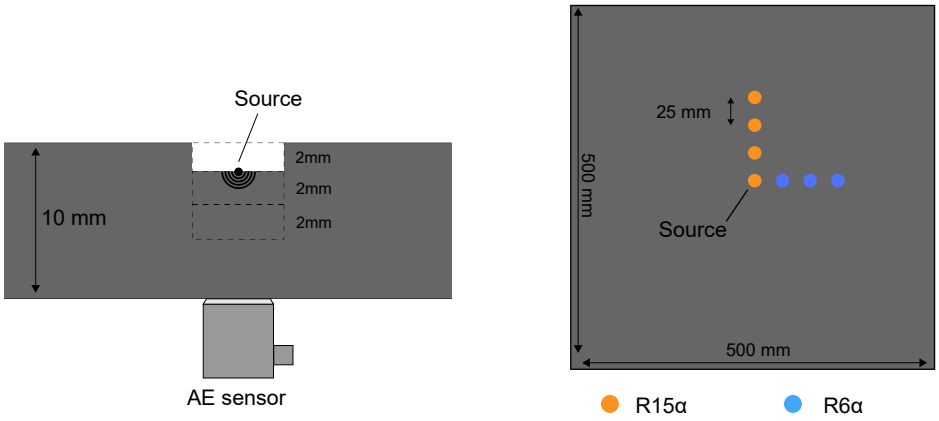

(a) Cross section of the sample

(b) sensor layout (bottom view)

Figure 2. Experimental set-up

An experimental set-up was designed to validate the findings from the numerical study. Figure 2 shows a schematic representation of the configuration of the transducers on the 500 mm x 500 mm x 10mm s420 steel specimen. The acoustic response of the specimen was measured with three R6α 60 kHz resonant sensors and four R15α 150 kHz resonant sensors manufactured by Physical Acoustics. These sensors were chosen for their sensitivity in their respective operating ranges so as to maintain high sensitivity over the entire frequency range of interest. The sensors were arranged in linear arrays with a spacing of 25 mm on the underside of the specimen. The characteristics of sensors and applied filters are listed in table II. A silicon-based couplant was used to ensure signal transmission to the sensors held in place by magnetic fasteners. Each sensor was connected to a dedicated AEP5 preamplifier (Vallen Systeme) set to a gain of +40 dB. In this configuration, the 3 dB bandwidth of the preamplifier stretches from 2.5 kHz to 2.4 MHz. The measurements were recorded using an AMSY-6 digital multi-channel measurement system (Vallen Systeme).The laboratory setup with the aforementioned equipment is shown in figure 3. Damage-related signals were simulated by means of a Hsu-Nielsen source (pencil-lead breaks) in accordance with ASTM E2374-16 guidelines [33].

An artificial damage with a depth of 2 mm and a diameter of 15 mm was introduced into the sample using an end mill as shown in figure 3. The depth of the artificial damage was increased in 2 mm increments before repeating 30 pencil-lead break tests. This repetition is needed in order to average out the variability in individual pencil-lead breaks and obtain more representative data.

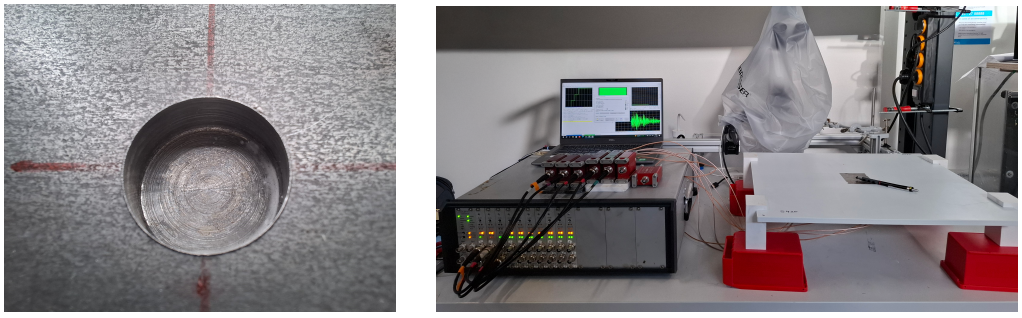

(a) artificial 4 mm depth defect (top view)

(b) Full laboratory set-up

Figure 3. Experimental set-up and artificial damage used during the experiments

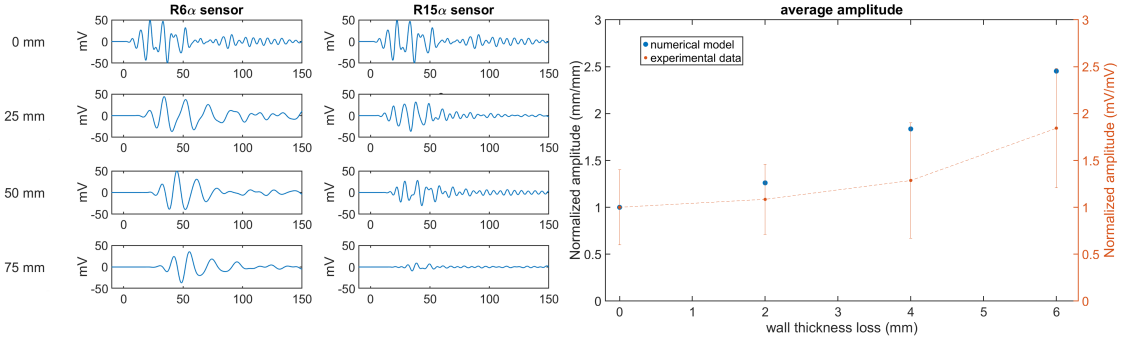

(a) AE event captured captured by the sensor array

(b) Average normalized signal amplitude for different damage depths for numerical and experimental results

Figure 4. results from the numerical model and experimental campaign

RESULTS

The experimental data show a significant amount of signal related to boundary reflections. The signals considered in this research were limited to the first signals arriving at each individual sensor for every pencil lead break; this is done to avoid taking into account reflections in the analysis. In order to reduce the effect of the variability of the pencil-lead breaks and the coupling conditions of the sensors, the average was taken over all AE events and different sensors. A typical AE signal as it propagates away from the source is shown in figure 4 a. The onset of the signals is time shifted to show the difference in arrival time caused by the wave propagation. The results from the numerical model indicate an increase in signal amplitude measured on the side opposite to the damage as the depth of the damage increases. The average signal amplitudes, normalized with respect to the average intact amplitude for both the numerical model and the experimental data are shown in figure 4 b for each increment of wall thickness loss. It can be seen that the average signal amplitude increases by 185% and 240% at a wall thickness loss of 6 mm for the experimental data and the numerical model data, respectively. The average amplitude of the signals captured by all of the sensors as the damage depth increases follows a similar trend to that of the numerical model.

DISCUSSION

Regarding the variability of the method presented above, three main sources of variability of the measured amplitudes were identified in this investigation. The first source is the coupling variation of the sensors. As the sensors had to be removed before machining the artificial damage and placed back on the specimen, it is to be expected that some variability is introduced. The exact coupling conditions can not be perfectly reproduced. The second source of variability is related to the sensor transfer function. Even though sensors of the same type were used, their manufacture can leave differences in the frequency response of each sensor. The third source of variability comes from the repeatability of the artificial AE source. Imperfections in the surface of the specimen and the material of the pencil lead can lead to variations in the source signal used to evaluate the response of the specimen.

The variability of the AE source can be dealt with by performing multiple repetitions of the test and averaging the results. The coupling variability of the sensors and the variability of their transfer functions can be overcome by averaging the results of different sensors, thereby reducing bias that may come from individual coupling conditions and transfer functions for any one sensor. By averaging out some of these variability sources, as performed in this study, the underlying trends can become more apparent.

CONCLUSIONS AND FUTURE WORK

The acoustic response of a carbon steel plate under different degrees of damage has been numerically and experimentally investigated. Corrosion-induced progressive wall thickness loss was artificially introduced in a steel plate equipped with AE sensors. Artificial AE sources were used to study the response of the specimen. The numerical study used a finite element model of the same plate with increasing damage at its center under high-frequency AE excitation. A correlation has been found between the loss in wall thickness and the average signal amplitude for a source located at the location of the damage. The behavior observed in the numerical model can also be observed in the experimental data.

In future work, it would be recommended to involve the correction of the signal amplitudes with other signal characteristics to develop a robust method to determine wall thickness loss. In order to deal with the variability, similar experiments with a more controlled, repeatable source would be recommended. Additionally, correcting for the transfer function of the sensors would allow for more consistent results. Finally, the verification of the aforementioned trends under accelerated corrosion conditions would be a valuable investigation.

FUNDING

This study was funded through the European Defense Fund (EDF) under grant agreement 101103257 dTHOR—EDF-2021-NAVAL- R-2.

REFERENCES

1. Emi, H., A. Kumano, N. Baba, N. Yamamoto, Y. Nakamura, and H. Shiihara. 1991. "A Study on Life Assessment of Ships and Offshore Structures," *Journal of the Society of Naval Architects of Japan*, 1991:443–454, ISSN 1884-2070, doi:10.2534/jjasnaoe1968.1991.443.
2. Kang, J., L. Sun, and C. G. Soares. 2019. "Fault Tree Analysis of floating offshore wind turbines," *Renewable Energy*, 133:1455–1467, ISSN 09601481, doi:10.1016/j.renene.2018.08.097.
3. Drumond, G. P., I. P. Pasqualino, B. C. Pinheiro, and S. F. Estefen. 2018. "Pipelines, risers and umbilicals failures: A literature review," *Ocean Engineering*, 148:412–425, ISSN 00298018, doi:10.1016/j.oceaneng.2017.11.035.
4. American Bureau of Shipping (ABS). 2016. "Guidance Notes on Structural Monitoring Using Acoustic Emissions," Tech. rep., American Bureau of shipping.
5. (DNV-GL), D. N. V. 2022. "Rules for Classification. Part 6 Additional Class Notations Chapter 9 Survey Arrangements," Tech. rep., DNV-GL.
6. Bureau Veritas. 2023. *Classification and survey*, Bureau Veritas, vol. Part A.
7. Pahlavan, P. L., J. Paulissen, R. Pijpers, H. Hakkesteegt, R. Jansen, R. J. Acoustic, and P. L. Pahlavan. 2014, "Acoustic Emission Health Monitoring of Steel Bridges," .
8. Nohal, L., P. Mazal, F. Vlasic, and M. Svobodova. 2019. "Acoustic Emission Response to Erosion-Corrosion and Creep Damage in Pipeline Systems," *Procedia Structural Integrity*, 23:227–232, ISSN 24523216, doi:10.1016/j.prostr.2020.01.091.
9. Calabrese, L. and E. Proverbio. 2020. "A Review on the Applications of Acoustic Emission Technique in the Study of Stress Corrosion Cracking," *Corrosion and Materials Degradation*, 2:1–33, doi:10.3390/cmd2010001.
10. Djeddi, L., R. Khelif, S. Benmedakhene, and J. Favergeon. 2013. "Reliability of Acoustic Emission as a Technique to Detect Corrosion and Stress Corrosion Cracking on Prestressing Steel Strands," *International Journal of Electrochemical Science*, 8:8356–8370, ISSN 14523981, doi:10.1016/S1452-3981(23)12894-X.
11. Calabrese, L., L. Bonaccorsi, M. Galeano, E. Proverbio, D. D. Pietro, and F. Cappuccini. 2015. "Identification of damage evolution during SCC on 17-4 PH stainless steel by combining electrochemical noise and acoustic emission techniques," *Corrosion Science*, 98:573–584, ISSN 0010938X, doi:10.1016/j.corsci.2015.05.063.
12. Kalteremidou, K.-A., D. G. Aggelis, D. V. Hemelrijck, and L. Pyl. 2021. "On the use of acoustic emission to identify the dominant stress/strain component in carbon/epoxy composite materials," *Mechanics Research Communications*, 111:103663, ISSN 00936413, doi:10.1016/j.mechrescom.2021.103663.
13. Yuyama, S., T. Kishi, and Y. Hisamatsu. 1984. "Fundamental Aspects of AE Monitoring on Corrosion Fatigue Processes in Austenitic Stainless Steel," *Journal of materials for energy systems*, 5.
14. Wu, K., F. Briffod, K. Ito, I. Shinozaki, P. Chivavibul, and M. Enoki. 2019. "In-Situ Observation and Acoustic Emission Monitoring of the Initiation-to-Propagation Transition of Stress Corrosion Cracking in SUS420J2 Stainless Steel," *MATERIALS TRANSACTIONS*, 60:2151–2159, ISSN 1345-9678, doi:10.2320/matertrans.MT-MAW2019004.
15. Jirarungsatian, C. and A. Prateepasen. 2010. "Pitting and uniform corrosion source recognition using acoustic emission parameters," *Corrosion Science*, 52:187–197, ISSN 0010938X, doi:10.1016/j.corsci.2009.09.001.
16. Liu, G., S. Wang, Y. Xie, X. Tian, D. Leng, R. Malekain, and Z. Li. 2018. "Damage detection of offshore platforms using acoustic emission analysis," *Review of Scientific Instruments*, 89, ISSN 0034-6748, doi:10.1063/1.5053735.

17. Drummen, I., L. Rogers, A. Benhamou, R. Hageman, and K. S. Marin. 2019. “Hull Structure Monitoring of a New Class of US Coast Guard Cutters,” *ASNE Technology*.
18. Ángela Angulo, J. Tang, A. Khadimallah, S. Soua, C. Mares, and T.-H. Gan. 2019. “Acoustic Emission Monitoring of Fatigue Crack Growth in Mooring Chains,” *Applied Sciences*, 9:2187, ISSN 2076-3417, doi:10.3390/app9112187.
19. Riccioli, F., S. Alkhateeb, A. Mol, and L. Pahlavan. 2024. “Feasibility assessment of non-contact acoustic emission monitoring of corrosion-fatigue damage in submerged steel structures,” *Ocean Engineering*, 312:119296, ISSN 00298018, doi:10.1016/j.oceaneng.2024.119296.
20. Vasagar, V., M. Hassan, A. Abdullah, A. Karre, B. Chen, K. Kim, N. Al-Qahtani, and T. Cai. 2024. “Non-destructive techniques for corrosion detection: A review,” *Corrosion Engineering Science and Technology*, 59:56–85, doi:10.1177/1478422X241229621.
21. Zima, B., K. Woloszyk, and Y. Garbatov. 2022. “Corrosion degradation monitoring of ship stiffened plates using guided wave phase velocity and constrained convex optimization method,” *Ocean Engineering*, 253, doi:10.1016/j.oceaneng.2022.111318.
22. Zima, B., E. Roch, and J. Moll. 2024. “Nondestructive corrosion degradation assessment based on asymmetry of guided wave propagation field,” *Ultrasonics*, 138:107243, ISSN 0041624X, doi:10.1016/j.ultras.2024.107243.
23. Chew, D., B. Masserey, and P. Fromme. 2021. “High-Frequency Guided Waves for Corrosion Thickness Loss Monitoring,” *Journal of Nondestructive Evaluation, Diagnostics and Prognostics of Engineering Systems*, 4, doi:10.1115/1.4048179.
24. Nicard, C., M. Farin, E. Moulin, D. Balloy, and I. P. Serre. 2023. “Monitoring of generalised corrosion: Ultrasonic coda wave interferometry technique applied to steel corrosion in aqueous NaCl solutions,” *Materials Chemistry and Physics*, 305:127908, ISSN 02540584, doi:10.1016/j.matchemphys.2023.127908.
25. Reed, N. and J. Corcoran. 2024. “Passive wall thickness monitoring using acoustic emission excitation,” *NDT & E International*, 148:103241, ISSN 09638695, doi:10.1016/j.ndteint.2024.103241.
26. Silionis, N. E. and K. N. Anyfantis. 2023. “On the Detection of Thickness Loss in Ship Hull Structures Through Strain Sensing,” pp. 207–216, doi:10.1007/978-3-031-07258-1_22.
27. Doyle, J. F. 2021. *Wave Propagation in Structures*, Springer International Publishing, ISBN 978-3-030-59678-1, doi:10.1007/978-3-030-59679-8.
28. Peng, H., G. Meng, and F. Li. 2009. “Modeling of wave propagation in plate structures using three-dimensional spectral element method for damage detection,” *Journal of Sound and Vibration*, 320:942–954, ISSN 0022460X, doi:10.1016/j.jsv.2008.09.005.
29. Pahlavan, L., C. Kassapoglou, and Z. Gürdal. 2013. “Spectral formulation of finite element methods using Daubechies compactly-supported wavelets for elastic wave propagation simulation,” *Wave Motion*, 50:558–578, ISSN 01652125, doi:10.1016/j.wavemoti.2012.12.006.
30. Komatitsch, D. and J. Tromp. 1999. “Introduction to the spectral element method for three-dimensional seismic wave propagation,” *Geophysical Journal International*, 139:806–822, ISSN 0956540X, doi:10.1046/j.1365-246x.1999.00967.x.
31. Komatitsch, D., C. Barnes, and J. Tromp. 2000. “Simulation of anisotropic wave propagation based upon a spectral element method,” *GEOPHYSICS*, 65:1251–1260, ISSN 0016-8033, doi:10.1190/1.1444816.
32. Kim, Y., S. Ha, and F.-K. Chang. 2008. “Time-Domain Spectral Element Method for Built-In Piezoelectric-Actuator-Induced Lamb Wave Propagation Analysis,” *AIAA Journal*, 46:591–600, ISSN 0001-1452, doi:10.2514/1.27046.
33. ASTM. 2021, “ASTM E2374-16 Standard Guide for Acoustic Emission System Performance Verification,” doi:10.1520/E2374-16R21.